Singaporean Journal of Scientific Research(SJSR)
Journal of Selected Areas in Microelectronics (JSAM)
Vol.8.No.2 2016 Pp.73-80
available at :www.iaaet.org/sjsr
Paper Received : 08-03-2016
Paper Accepted: 19-04-2016
Paper Reviewed by: 1.Prof. Cheng Yu 2. Dr.M. Akshay Kumar
Editor : Dr. Chu Lio

A SINGLE SWITCH FULLY SOFT- SWITCHING ISOLATED DC-DC CONVERTER FOR RENEWABLE APPLICATION

MURALI ,MANOHARAN,MURUGESAN
PG Scholar
Department of Electrical and Electronics Engineering
Government College of Engineering, Salem ,Tamilnadu, India

A . RUBY MEENA
Assistant Professor
Department of Electrical and Electronics Engineering Government College of Engineering, Salem
Tamilnadu, India

ABSTRACT

This paper proposes a soft switching techniques by using the isolated DC-DC converter in a single switch. To analysis and design of a new DC-DC converter applied for the applications, such as photovoltaic module-integrated converter (MIC) systems, portable fuel cell systems and vehicle inverters. The proposed topology, based on the soft switching technique, uses only one switch to step up the mains voltage with high gain The proposed converter has able to offer reduced cost and high power density in boost application due to the following features because of the switch has turn on by Zero current switching and turn-off by Zero voltage switching and Zero current switching turn-off and diodes regardless of voltage and load variation and low rated lossless snubber and reduced volume of transformer comparing flyback converter due to low magnetizing current.

Index Terms—*Isolated step up DC-DC converter, single switch , soft switching , MATLAB*

I. Introduction

Isolated step-up dc-dc converters are used in many application, such asphotovoltaic module-integrated converter (MIC) systems, portable fuel cell systems[1] and hybrid vehicle inverters where high efficiency, high power density and low cost are required[4]. A photovoltaic system is a system which uses one or more solar panels to convert solar energy into electricity. In order to smaller input current ripple, lower diode voltage rating and lower transformer turns ratio, the current-fed isolated converter is better suited for step-up applications. The current-fed isolated converter has two types: passive-

clamped[5] and active-clamped[8] The passive-clamped current-fed converter has simple structure and small switch count, but suffers from excessive power losses dissipated in the RCD snubber and associated with hard switching of main switch. Active-clamped current-fed converters have actively been developed based on three methods :push-pull[5] ,full-bridge[6] and half-bridge[11]. They achieve not only lossless clamping of voltage spikes caused by transformer leakage inductance but also zero-voltage switching (ZVS)turn on of the switches. The effect of the reverse-recovery-related problems become more significant for high switching frequency at high power level. However, they can't be expected to achieve high efficiency and low cost in relatively low power application since they need at least two or more switches and corresponding gate driver circuits.

Isolated converters with reduced switch count have been proposed for low power application [8]. Isolated dc-dc converter swith one main switch and one clamp switch achieves ZVS turn on of switches, but switches are turned off with hard switching[11]. Isolated single switch dc-dc converters are more attractive to achieve low cost Z-source converter and flyback converter[15] are hard switched at both turn-on and turn-off instants. Frequency-controlled flyback converter and series-connected forward-flyback converter achieve zero-current switching (ZCS)turn-on of switch, but the switch is hard switched at turn-off instant. The above mentioned single switch topologies have increased transformer volume since magnetizing inductor is used for energy transfer . An isolated single-switch resonant converter achieves[17] both ZCS turn-on and ZCS turn-off of switch, but need high transformer turn ratio for step-up application due to low voltage gain and hence is not suited to boosted application.

This paper proposes a soft switching techniques by using the isolated DC-DC converter in a single switch.. The proposed converter has the following features: 1) ZCS turn-on and ZVS turn-off of switch regardless of voltage and load variation 2) ZCS turn-off of all diodes leading to negligible voltage surge associated with the diode reverse recovery 3) small input current ripple due to CCM operation 4) transformer volume are reduced due to low magnetizing current 5) low rated lossless snubber , which makes it possible to achieve high efficiency and low cost for step-up application.

II. PROPOSED CONVERTER

Fig.1 shows the circuit of the proposed converter. The proposed converter has the components of input filter inductor *Li*, switch *S*, a lossless snubber should include capacitor *Cs*, inductor *Ls*, and diodes *Ds1* and *Ds2*, and clamp capacitor *Cc* at the primary side and *Lr-Cr* series resonant circuit and diodes *D1*and *D2*at the secondary side. The lossless snubber will possible to achieve ZVS turn-off of switch as well as clamp the voltage spikes of the switch by leakage inductance.

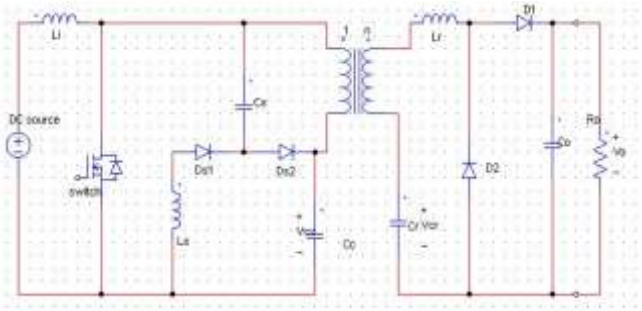

Fig 1: Circuit diagram of proposed dc-dc converter

Also, the Lr-Cr series resonant circuit makes it possible to achieve ZCS turn-off of diodes. Fig. 2 shows three resonance operations according to the variations of resonant frequency fr1which is expressed as in (1): the above-resonance operation (DTs< 0.5Tr1), the resonance operation (DTs= 0.5Tr1), and the below-resonance operation (DTs> 0.5Tr1).

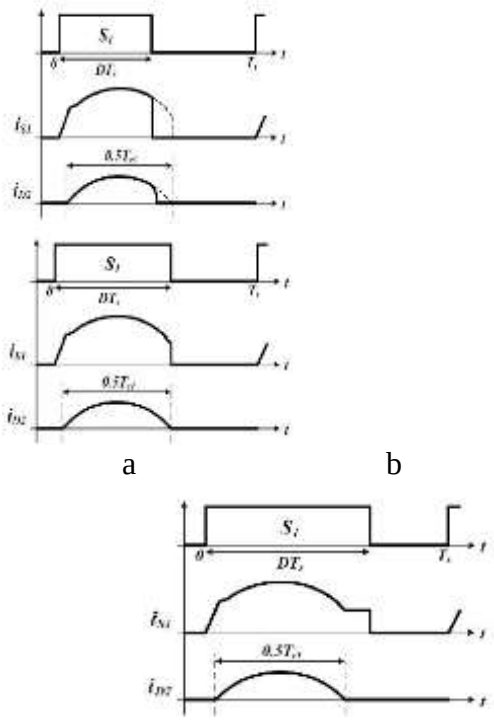

Fig. 2. Comparison of switch and diode current waveform according to variation of switching frequency: (a) Above-resonance operation (DTs < 0.5Tr1), (b) Resonance operation (DTs = 0.5Tr1), and (c) Below-resonance operation (DTs > 0.5Tr1).

$$fr1 = \frac{1}{Tr1} = \frac{1}{2\pi\sqrt{LrCr}} \qquad (1)$$

It can be seen from Fig. 2 that the total switching losses are smaller for the below-resonance operation since both switch turn-off current and diode di/dt of the below-resonance operation are smaller than them of the above-resonance operation. Therefore, the below-resonance operation is chosen for the proposed converter.

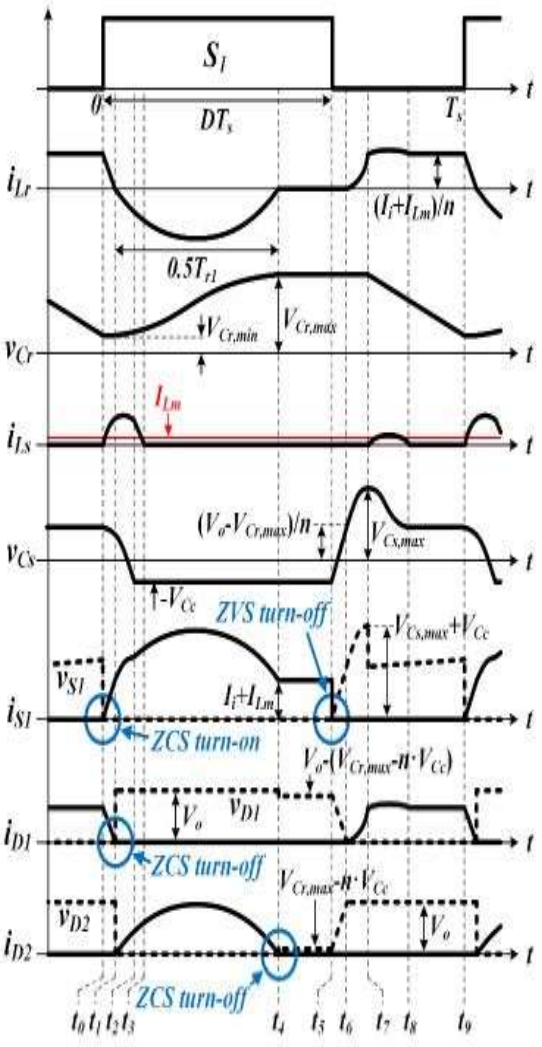

Fig 3. schematic operating waveforms to illustrate the operation of ZVS&ZCS

A. OPERATING PRINCIPLE

Figs. 3 and 4 show the waveforms and operationing states of the proposed converter in the below-resonance operation(DTs > 0.5Tr1), respectively. In order to design the analysis of the steady-state operation, it is assumed that the input filter and magnetizing inductances are large enough so that they can be treated as constant current sources during a switching period. It is also assumed that clamp and output capacitances are large enough so that they can be treated as constant voltage sources during a switching period. The voltage *VCc* across the clamp capacitor is the same as the input voltage *Vi*. In the

below-resonance operation, nine modes exist within *Ts*.

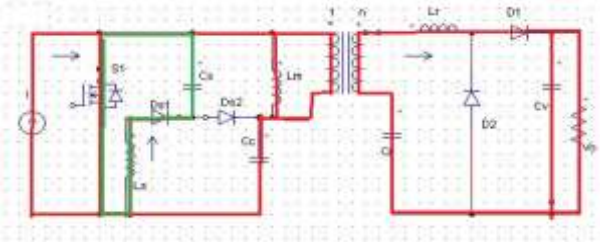

Mode 1: (T0 - T1)

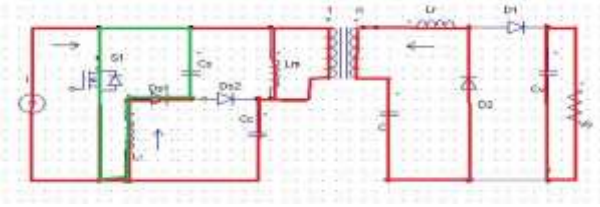

Mode 2: (T1 –T2)

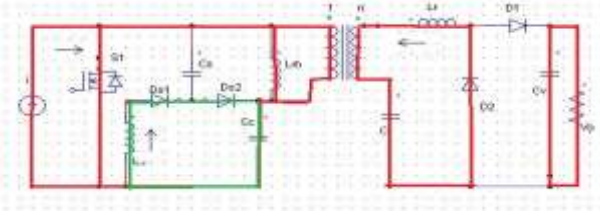

Mode 3: (T2 –T3)

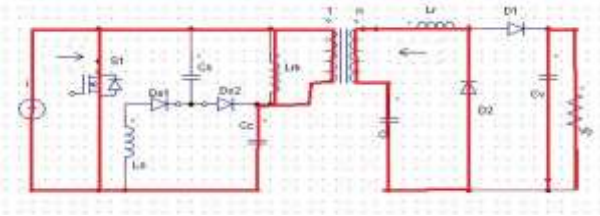

Mode 4: (T3 –T4)

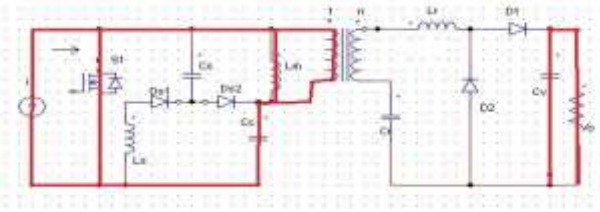

Mode 5: (T4 –T5)

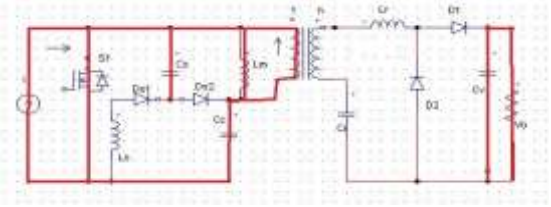

Mode 6: (T5 –T6)

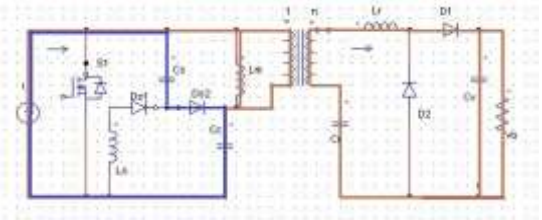

Mode 7:(T6-T7)

Mode 1: (T0 - T1)

This mode begins when switch *S1* is turned ON. Equivalent circuit of this mode is shown in Fig. 5(a). *Ls* and *Cs* start resonating and resonant current *iLs* flows through *Ls*, *Ds1*, *Cs*, and *S1*. The voltage and current of resonant components are determined, respectively, as follows:

$$i(t) = Vcs(to)\sqrt{\frac{Cs}{Ls}}\sin(\omega r(t-to)), to < t < t2 \quad (2)$$

$$i(t) = Vcs(to)\cos(\omega r(t-to)), to < t < t2 \quad (3)$$

Where, $\omega r2 = \frac{1}{\sqrt{LsCS}}$ Since induced voltage *VCr,min-nVCc-Vo* across *Lr* makes time interval from *t0* to *t1* very short, current *iLr* appears to decrease almost linearly. Current through *S1* increases with the slope of *iLr*, resulting in ZCS turn-on of *S1*. The turn-on loss of switch associated with energy stored in MOSFET's output capacitance is negligible in this low input voltage application [27]-[29]. This mode ends when current *iLr* reaches 0A. It is noted that diode *D1* is turned OFF under ZCS condition

Mode 2: (T1 –T2)

This mode begins when current *iLr* changes its direction. Equivalent circuit of this mode is shown in Fig. 5(b). *Lr* and *Cr* start resonating and resonant current *iLr* flows through *Lr*, *Cr*, and *D2*. The voltage and current of resonant components are determined, respectively, as follows:

$$i(t) = (Vcs - nVcs)\sqrt{\frac{Cr}{Lr}}\sin(\omega r(t-t1)), t1 < t < t4 \quad (4)$$

$$V(t) = nVcc - (nVcc - Vc\min)\cos(\omega r(t-t1)), t1 < t < t4 \quad (5)$$

Mode 3: (T2 –T3)

This mode begins when diode *Ds2* is turned ON. From this time Current *iLs* is determined by following equation, and this mode stops when current *iLs* reaches 0A.

$$I(t) = -\frac{Vcc}{Ls}(t1-t2) + Is(t2), t5 < t < t6 \quad (6)$$

Mode 4: (T3 –T4)

The *Lr-Cr* resonance keeps on during this mode and ends when current *iLr* reaches 0A. Under ZCS condition diode *D2 is* turned OFF.

Mode 5: (T4 –T5)

During this mode a constant current flows through *S1* whose value is the sum of the input current *Ii* and the magnetizing current *ILm*.

Mode 6: (T5 –T6)

The mode begins when *S1* is turned OFF. Then, *Ii + ILm* flows through *Cs, Ds2*, and *Cc*. Voltage across snubber capacitor *Cs* which is determined by the following equation increases linearly with the slope of *(Ii+ILm)/Cs*, resulting in ZVS turn-off of *S1*.

$$I(t) = -\frac{Ii + Ilm}{Cs}(t - t5) - Vcc, t6 < t < t7 \quad (7)$$

Mode 8:(T7-T8)

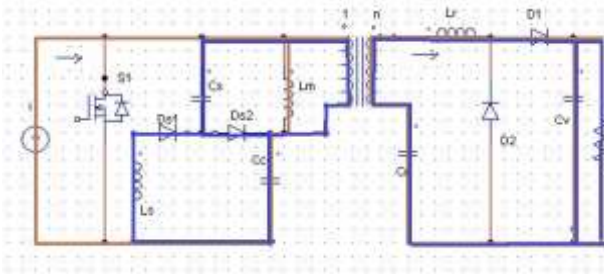

Mode 9:(T8-T9)

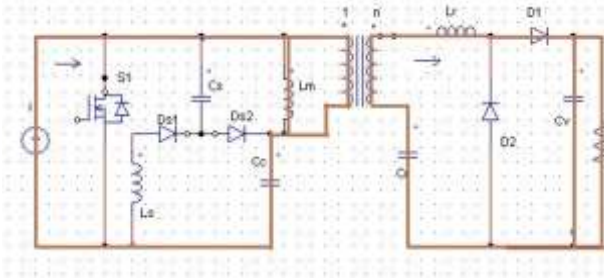

Mode 7:(T6-T7)

This mode begins when diode *D1* is turned ON. *Lr* and *Cs* starts conduction for resonating and resonant current *iLr* flows through *Cs*, *Ds2*, *Lr*, *D1*, and *Cr*. Assuming that *Cs* << *n2Cr*, *vCr* can be considered constant, and resonance frequency can be determined by *Cs* and *Lr*. Therefore, the voltage and current of resonant components are determined, as follows:

$$I(t) = (Ii + Ilm)[1 - \cos(\omega r(t - t6))], t6 < t < t7 \quad (8)$$

$$V(t) = \frac{Ii + Ilm}{n}\sqrt{\frac{Lr}{Cs}}\sin(\omega r(t - t6)) + \frac{Vo - Vcc}{n}, t6 < t < t7 \quad (9)$$

Mode 8:(T7-T8)

This mode begins when diode *Ds1* is turned ON as shown in the fig *Ls, Cs, Lr* and *Cr* start resonating and resonant current *iLr* flows through *Ls, Ds1, Cs, Cc, Lr, D1*, and *Cr*.

This mode ends when current *iLs* reaches 0A.

Mode 9:(T8-T9)

Switch *S1* is to be turn-off condition, and the sum of the input current and magnetizing current is being transferred to the secondary. Current *iD1* is equal to *(Ii+ILm)/n*. This mode ends when switch *S1* is turned ON.

The average current of magnetizing inductor *Lm* is equal to average current of snubber inductor *Ls* since *ILs,avg = IDs2,avg* and *IDs2,avg = ILm,avg*. Therefore, it should be noted that transformer core volume of the proposed converter is much smaller compared to that of the flyback based converter since *ILs,avg* (= *ILm,avg*) can be designed to be small.

B. Voltage GainExpression

To obtain voltage gain of the proposed soft switching

DC-DC converter, it is assumed that voltage across *Cc*is constant and magnetizing current is eliminated during the switching period *Ts*.

1) Below-resonance operation (DTs > 0.5Tr1):

From the average current of diode *D2* is identical to the average load current in the steady-state condition.

The maximum voltage of the resonance capacitor Vcr,min can be obtained as,

$$Vcr, \min = nVcc - \frac{Vo}{2CrfsRo} \quad (10)$$

The maximum voltage of the resonant capacitor VCr,max can be obtained by,

$$Vcr, \max = nVcc + \frac{Vo}{2CrfsRo} \quad (11)$$

The time interval from t6 to t7 in Fig. 3 is quarter the Lr-Cs
resonant frequency and determined by

$$t7 - t6 = \frac{\pi}{2\omega s} \qquad (12)$$

The voltage gain can be obtained by

$$\frac{Vo}{Vi} = \frac{n + B}{1 - D - A} \qquad (13)$$

Where,

$$A = \frac{\pi fs}{2\omega s} \quad \&$$

$$B = \frac{Cs(2CsfsRo - 1)}{2nCr}$$

C. Design Procedure

1) Choose average value of snubber inductor current ILs,avg:ILs,avg should be as small as possible in order to minimize conduction loss of the snubber components and magnitude of the magnetizing current. However, if *Cs* is chosen to be small to reduce conduction loss of the snubber components the voltage rating of the switch increases, as shown in (9), resulting in high conduction loss of the switch. Therefore, considering tradeoff between conduction losses of the switch and snubber components, *ILs,avg* is chosen to be around 3% of average input current, which is expressed as

Ils,avg = 0.03 Ii,avg = 0.27A

2) Determine values of n, Lr, and Cr: In order to simplify the design procedure, the voltage gain can be approximated as

$$\frac{Vo}{Vi} = \frac{n}{1 - D} \qquad (11)$$

From the equation ,the below resonance operation is chosen for the proposed converter due to smaller switch turn off current and diode di/dt so that the minimum duty cycle for the below resonance operation can be obtained as

$$D\min = \pi fs\sqrt{LrCr} \qquad (12)$$

In the transformer ratio n has been chosen as 1:5 is considering to turn off condition loss and switching loss of switch S.

3) Determine value of Ls: Snubber inductance Ls should be designed to minimize reverse-recovery effects of snubber diodes Ds1 and Ds2.from that the reverse recovery time of the diodes the snubber inductance Ls is to be chosen.

III SIMULATION RESULTS

The proposed converter has been built and tested to verify the proposed concept. Component ratings and selected devices of the proposed converter are listed in Table I. that current ratings of the snubber components are much lower than Leakage inductance of the transformer is used as the resonant inductance

Output Voltage: Vo = 500Volts
Input Voltage: Vin =45 Volts
Output Power: Po = 250 W
Switching Frequency: fs = 100 kHz
Duty cycle; D = 0.65
Load Resistor: R = 570 ohm

The following components were used to implement the simulation of the proposed boost converter:

Filter inductor Li =100mh
Snubber inductor Ls = 5mh
Snubber capacitor Cs = 16nF
Resonant capacitor Cr = 560nF
Resonant capacitor Co = 1µF
Clamp capacitor Cc = 82µF
Snubber capacitor Cs =16nF

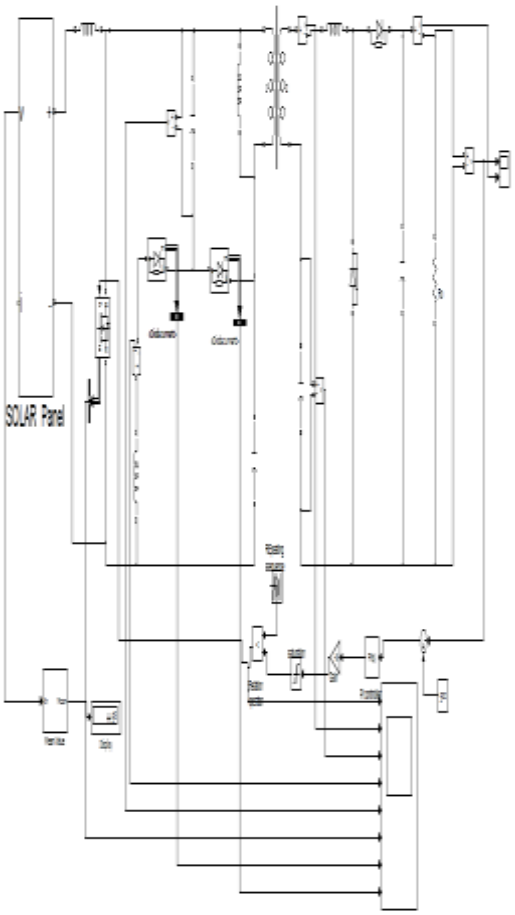

Fig.5 Simulation circuit of proposed converter in MATLAB

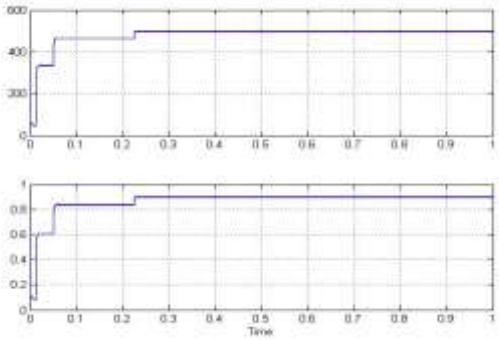

Fig.6 Output Voltage & current waveform duty cycle of 0.65

The output voltage and current waveform is above it has ben chosen as the input voltage as 45volt with the solar panel. and has the output voltage as the 500volts with the duty cycle of 0.65 and with respective element of the passive components has been mentioned above. Thereby switching losses are greatly reduced. zvs is achieved by resonant tank Ls and C which are very small in values.

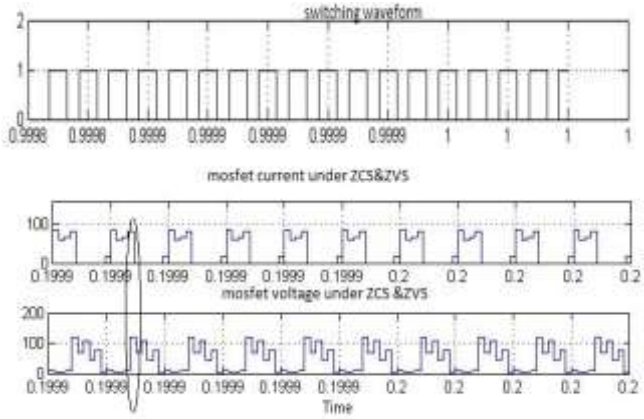

Fig 7: the switching current &voltage waveform for the condition of under ZVS and ZCS

It show experimental waveforms at full load condition when input voltage is 45V, respectively. Fig. 8 show that switch *S1* is turned ON with ZCS at both full and half load conditions. Fig. 8 show the experimental waveforms of switch *S1* at turn-off. In theory, *S1* is turned OFF with ZVS.

IV CONCLUSION

In this paper, a single-switch soft switch power converter with an energy-blocking diode has been designed for use in a solar energy generation system. The structure of the proposed converter is simpler and cheaper than other soft switch power converters, which require numerous components. The novel soft switch converter is analyzed, and performance characteristics are presented. A single switch soft-switched isolated converter was proposed for step-up application such as MIC, portable fuel cell systems and vehicle inverters. Improved features such as fully soft-switched characteristics of switch and diode, low rated lossless snubber and reduced transformer volume make the proposed converter achieve lower cost and higher power density compared to the conventional flyback based converter.

REFERENCES

[1] Q. Li, and P. Wolfs , “A review of the single phase photovoltaic module integrated converter topologies with three different dc

link configurations," IEEE Trans. Power Electron., vol. 23, no. 3, pp. 13201333, May. 2008.

[2] D. A. Ruiz-Caballero and I. Barbi, "A new flyback-current-fed push-pull DC-DC converter," IEEE Trans. Power Electron., vol. 14, no. 6, pp. 1056-1064, Nov. 1999.

[3] M. Nymand and M. A. E. Andersen, "High-efficiency isolated boost DC DC converter for high-power low-voltage fuel-cell applications," IEEE Trans. Ind. Electron., vol. 57, no. 2, pp. 505-514, Feb. 2010.

[4] F. J. Nome and I. Barbi, "A ZVS clamping mode-current-fed push–pull DC–DC converter," in Proc. IEEE Int. Symp. Ind. Electron., 1998, vol. 2,pp. 617-621

[5] R. Watson and F. C. Lee, "A soft-switched, full-bridge boost converter employing an active clamp circuit," in Proc. IEEE Conf. Power Electron.Spec. Conf. Rec., 1996, vol. 2, pp. 1948-1954.

[6] S. Han, H. Yoon, G. Moon, M. Youn, Y. Kim, and K. Lee, "A new active clamping zero-voltage switching PWM current-fed half-bridge converter," IEEE Trans. Power Electron., vol. 20, no. 6, pp. 1271-1279, Nov.2005.

[7] J. Kwon and B. Kwon, "High step-up active-clamp converter with inputcurrent doubler and output-voltage doubler for fuel cell power systems," IEEE Trans. Power Electron., vol. 1, no. 1, pp. 108-115, Jan. 2009.

[8] C.D. Davidson, "Zero Voltage Switching Isolated Boost Converter Topology," in Proc. IEEE 33rd Int. Telecommun. Energy Conf., Oct. 2011, pp. 1-8.

[9] G. Spiazzi, P. Mattavelli, and A. Costabeber, "High step-up ratio flyback converter with active clamp and voltage multiplier," IEEE Trans. Power Electron., vol. 26, no. 11, pp. 3205-3214, Nov. 2011.

[10] B. York, W. Yu, and J.-S. Lai, "Hybrid-frequency modulation for PWMintegrated resonant converters," IEEE Trans. Power Electron., vol. 28, no. 2, pp. 985-994, Feb. 2013.

[11] B. York, W. Yu, and J.-S. Lai, "An integrated boost resonant converter for photovoltaic applications," IEEE Trans. Power Electron., vol. 28, no. 3, pp. 1199-1207, Mar. 2013.

[12] F. Evran and M. T. Aydemir, "Z-source-based isolated high step-up converter," IET Power Electron., vol. 6, no. 1, pp. 117-224, Jan. 2013.

[13] F. Evran and M. T. Aydemir, "Isolated high step-up DC-DC converter with low voltage stress," IEEE Trans. Power Electron., vol. 29, no. 7, pp. 3591-3603, Jul. 2014.

[14] K. B. Park, C. E. Kim, G. W. Moon, and M.-J. Youn, "PWM resonant single-switch isolated converter," IEEE Trans. Power Electron., vol. 24, no. 8, pp. 1876-1886, Aug. 2009.

[15] J.-M. Kwon, W.-Y. Choi, and B.-H. Kwon, "Single-switch quasiresonant converter," IEEE Trans. Ind. Electron., vol. 56, no. 4, pp. 11581163, Apr. 2009.

[16] J.-H. Lee, J.-H. Park, and J. H. Jeon, "Series-connected forward-flyback converter for high step-up power conversion," IEEE Trans. Power Electron., vol. 26, no. 12, pp. 3629-3641, Dec. 2011.

[17] A. Emrani, E. Adib, and H. Farzanehfard, "Single-switch soft-switched isolated DC-DC converter," IEEE Trans. Power Electron., vol. 27, no. 4, pp. 1952-1957, Apr. 2012.

[18] M. Matsuo, T. Suetsugu, S. Mori, and I. Sasase, "Class DE currentsource parallel resonant inverter," IEEE Trans. Ind. Electron., vol. 46, no. 2, pp. 242-248, Apr. 1999. [28] Y. Ren, M. Xu, J. Zhou, and F. C. Lee, "Analytical loss model of power MOSFET," IEEE Trans. Power Electron., vol. 21, no. 2, pp. 310-319, Mar. 2006.

[19] T. J. Liang, R. Y. Chen, and J. F. Chen, "Current-fed parallel-resonant dc–ac inverter for cold-cathode fluorescent lamps with zero-current switching," IEEE Trans. Power Electron., vol. 23, no. 4, pp. 2206-2210, Jul. 200